Ferromagnetic properties of selectively Mn-doped (Ga,Mn)As quantum wells

Hye Jung Kim* and Kyung Soo Yi†
Department of Physics, Pusan National University, Busan 609-735, Korea
(Received 1 July 2009; revised manuscript received 28 August 2009; published 2 November 2009)

We investigate temperature dependence of spin-resolved subband structure and spontaneous magnetization for different doping profiles of magnetic impurities in diluted (Ga,Mn)As quantum well structures. The self-consistent hole subband energies and wave functions are determined by solving combined Schrödinger and Poisson equations numerically. We included the coupling effects among heavy-hole, light-hole, and split-off bands (six-band model) in our calculation and compared the result with the case of two-band model. We show that selective doping of magnetic ions in GaAs quantum well enhances the Curie temperature T_c significantly, but holes occupying light-hole subbands result to reduce spontaneous magnetization and hence the Curie temperature of the system. This reduction effect reveals more clearly near the $T \sim T_c$ hindering an increase in the Curie temperature in a selectively Mn-doped system.

DOI: 10.1103/PhysRevB.80.193201 PACS number(s): 75.75.+a, 75.50.Pp, 75.25.+z, 75.10.Lp

I. INTRODUCTION

Electrical control of magnetic properties of spintronics materials has drawn much attention over the past decades, primarily challenging to combine storage and processing of information at practical operation temperature. Diluted magnetic semiconductor (DMS) $Ga_{1-x}Mn_xAs$ reveals ferromagnetic phase at low temperature and has become a prototypical ferromagnetic semiconductor. Its magnetic properties can be tuned by varying carrier concentration, since ferromagnetic ordering between magnetic impurities is mediated by carriers.[1,2] However, device applications of DMS material have been limited due to low values of ferromagnetic transition temperature T_c. Recently, its T_c was reached to maximum 185 K ($x \approx 12\%$) by post-growth low-temperature annealing,[3] but it is still lower than room temperature. For a quantum well (QW) structure, the distributions of magnetic impurities and charge carriers can be controlled by the well parameters such as the width and the depth of the QW or doping profiles. It was suggested that T_c would be tuned by varying the parameters of the host semiconductor and QW geometry[4,5] or doping profiles of magnetic impurities (in two-band model).[6] It is also reported that T_c is high up to 250 K in Mn δ-doped GaAs/Be-doped AlGaAs heterostructure[7] and that T_c can be tuned with the width of AlAs layers in $Ga_{1-x}Mn_xAs$/AlAs multiple QWs.[8] Hybrid structures of ferromagnet and semiconductor are promising for combining properties needed to overcome the limits of conventional information devices. One can imagine various hybrid structures formed in a DMS $Ga_{1-x}Mn_xAs$ QW doped selectively with Mn impurities.[6]

In this Brief Report, we show self-consistent spin-resolved subband structure and temperature dependence of spontaneous magnetization of two-region selectively Mn-doped $Ga_{1-x}Mn_xAs$ DMS QWs (see, for example, Fig. 1). We compare the results of two-band and six-band model calculations for three different Mn-doping profiles and study the connections between the magnetic properties and doping profiles of magnetic ions in the GaAs QW.

II. THEORY

Let us consider a structure, in which Mn ions are selectively doped in the GaAs region of (Al,Ga)As /GaAs/(Al,Ga)As QW (we take the z axis parallel to the given direction of the heterostructure). The Hamiltonian of a hole in the structure is given by

$$H = H_0 + v_{\text{s.c.}}(z) + v_{\text{xc}}^{\sigma}(z;\zeta) + H_{\text{ex}}^{\sigma}(z). \tag{1}$$

Here H_0 is the one-particle Hamiltonian of a hole in the one-dimensional confinement potential $V(z)$ of the QW. $v_{\text{s.c.}}(z)$ is the sum of the Hartree potential of free holes and the potential due to ionized magnetic (acceptor) impurities, and it should be determined self-consistently.[6] The itinerant two-dimensional (2D) hole concentration is $n_{2\text{D}} = \alpha(x_{\text{eff}}N_0) \times 2d_{\text{Mn}}$, where x_{eff} is the effective mole fraction of uncompensated Mn moments and N_0 is the number of cation sites per unit volume. And α is the "doping efficiency" denoting the density ratio of uncompensated Mn impurities and itinerant carriers.[9] $v_{\text{xc}}^{\sigma}(z;\zeta)$ denotes a spin-dependent exchange-correlation potential[10] and $H_{\text{ex}}^{\sigma}(z)$ is the exchange interaction Hamiltonian between Mn spins $\vec{S}$ and hole spins $\vec{\sigma}$, which is approximated by $H_{\text{ex}}^{\sigma}(z) = \vec{\sigma} \cdot \langle \vec{S} \rangle x_{\text{eff}} J_{pd} \Sigma_{\vec{R}} \delta(\vec{r} - \vec{R})$.[6,9,11] Here $\vec{r}$ and $\vec{R}$ are coordinates of a hole and cations, respectively, J_{pd} is exchange coupling constant. In order to calculate the subband structure of holes in the valence band of the QW, we write the subband wave function of a hole in the form

$$\Psi_{\ell}(\vec{r}) = \sum_{j=1}^{6} e^{i(k_x x + k_y y)} \varphi_{j\ell}(z) u_{j0}(\vec{r}). \tag{2}$$

Here indices j and ℓ denote the (spin-resolved) band index and subband quantum number, respectively, and u_{j0} are Bloch functions at $\vec{k}=0$ of the valence band, which consists of heavy-hole (hh), light-hole (lh), and split-off band states. Using the wave function of Eq. (2), we transform the Schrödinger equation of Hamiltonian H given by Eq. (1) into 6×6 matrix equation as follows:[12]

$$\sum_{i,j=1}^{6} \langle u_{j0}|H|u_{i0}\rangle \varphi_{i\ell}(z) = \sum_{i=1}^{6} E_{\ell} \varphi_{i\ell}(z). \tag{3}$$

Now one can evaluate $\{E_{\ell}, \varphi_{i\ell}\}$ numerically at finite temperature for a given Mn-doping profile using such a technique as the finite difference method.[13]

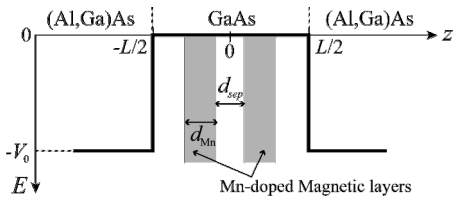

FIG. 1. Schematic diagram of selectively Mn-doped quantum well structure. L and V_0 denote the width and depth of the QW, respectively. Mn-doped regions are shaded in gray in the well. d_{Mn} indicates the width of each piece of selectively Mn-doped region.

The explicit matrix representations of Hamiltonian components of H in Eq. (3) are given as follows. First, the one-particle Hamiltonian H_0 is written as[12,14]

$$\begin{pmatrix} H_{\mathrm{hh}} & 0 & 0 & 0 & 0 & 0 \\ 0 & H_{\mathrm{lh}} & 0 & 0 & -H_{\mathrm{ls}} & 0 \\ 0 & 0 & H_{\mathrm{lh}} & 0 & 0 & H_{\mathrm{ls}} \\ 0 & 0 & 0 & H_{\mathrm{hh}} & 0 & 0 \\ 0 & -H_{\mathrm{ls}} & 0 & 0 & H_{\mathrm{so}} & 0 \\ 0 & 0 & H_{\mathrm{ls}} & 0 & 0 & H_{\mathrm{so}} \end{pmatrix} \tag{4}$$

where H_{hh}, H_{lh}, H_{ls}, and H_{so} are defined by

$$H_{\mathrm{hh}} = \frac{\hbar^2}{2m_0}\frac{\partial}{\partial z}[\gamma_1(z) - 2\gamma_2(z)]\frac{\partial}{\partial z} + V_0(z),$$

$$H_{\mathrm{ls}} = -\frac{\sqrt{2}\hbar^2}{m_0}\frac{\partial}{\partial z}\gamma_2(z)\frac{\partial}{\partial z},$$

$$H_{\mathrm{lh}} = \frac{\hbar^2}{2m_0}\frac{\partial}{\partial z}[\gamma_1(z) + 2\gamma_2(z)]\frac{\partial}{\partial z} + V_0(z),$$

$$H_{\mathrm{so}} = \frac{\hbar^2}{2m_0}\frac{\partial}{\partial z}\gamma_1(z)\frac{\partial}{\partial z} + \Delta + V_1(z). \tag{5}$$

Here $\gamma_i(z)(i=1,2,3)$ are Luttinger parameters, which describe the anisotropy of the valence band and they have direction dependence of the QW structure. Δ is the energy split of split-off band at $\vec{k}=0$, and $V_0(z)$ and $V_1(z)$ are confinement potentials of hh and lh bands and split-off band, respectively. Second, the exchange interaction Hamiltonian H_{ex}^{σ} can be represented as[15]

$$x_{\mathrm{eff}}N_0\beta\langle S_y\rangle \begin{pmatrix} \frac{1}{2} & 0 & 0 & 0 & 0 & 0 \\ 0 & \frac{1}{6} & 0 & 0 & \frac{\sqrt{2}}{3} & 0 \\ 0 & 0 & -\frac{1}{6} & 0 & 0 & -\frac{\sqrt{2}}{3} \\ 0 & 0 & 0 & -\frac{1}{2} & 0 & 0 \\ 0 & \frac{\sqrt{2}}{3} & 0 & 0 & -\frac{1}{6} & 0 \\ 0 & 0 & -\frac{\sqrt{2}}{3} & 0 & 0 & \frac{1}{6} \end{pmatrix}, \tag{6}$$

where $\beta=\langle\phi|J_{pd}(\vec{r})|\phi\rangle(\phi=X,Y,Z)$ is the p-d exchange integral. And we assume that the easy axis of (Ga,Mn)As is in the $\vec{y}$ direction (in-plane magnetization). The thermal average of Mn spins is given by $\langle S_y\rangle=-\frac{5}{2}B_{5/2}(\xi)$ where $B_S(x)$ is the standard Brillouin function and $\xi=-\frac{1}{2}J_{pd}[n_{\downarrow}(z)-n_{\uparrow}(z)]/k_BT$. We note that ξ is proportional to spin-polarized hole density $n_{\downarrow}(z)-n_{\uparrow}(z)$. Finally the potentials $v_{s.c.}(z)$ and v_{xc}^{σ} are described as a function of total hole density $n(z)$ or spin polarization $\zeta=\frac{n_{\downarrow}-n_{\uparrow}}{n_{\downarrow}+n_{\uparrow}}$ and they are added to diagonal components in the Hamiltonian matrix. In actual calculation of those potentials, we need areal concentrations of holes occupying each subband of the QW. At finite temperature T, we define the areal concentration n_{ℓ}^{2D} of holes occupying the ℓ^{th} subband of bottom energy E_{ℓ} as

$$n_{\ell}^{\mathrm{2D}} = \int_0^{\infty} m_{\ell}^{\mathrm{eff}}\rho_{\ell}^{\mathrm{2D}}(E)f(E)dE. \tag{7}$$

Here $\rho_{\ell}^{\mathrm{2D}}(E)=m_e/(2\pi\hbar^2)\theta(E_{\ell}-E)$ is the density of states of a 2D system and $f(E)$ is the Fermi-Dirac distribution function for holes. m_{ℓ}^{eff} is the ratio between electron mass m_e and effective mass of a hole in the ℓ^{th} subband state, which consists of a linear combination of hh, lh, and split-off band states:

$$m_{\ell}^{\mathrm{eff}} = \frac{\Sigma_{j=1}^{6} m_j|\varphi_{j\ell}(z)|^2}{m_e\Sigma_{j=1}^{6}|\varphi_{j\ell}(z)|^2}, \tag{8}$$

where m_j's indicate the effective masses of the valence band for bulk. For the case of GaAs, effective masses of hh, lh, and split-off bands are $m_{\mathrm{hh}}=0.5m_e$, $m_{\mathrm{lh}}=0.076m_e$, and $m_{\mathrm{so}}=0.145m_e$, respectively.[16] By integrating Eq. (7), one can write the 2D hole density n_{ℓ}^{2D} of the ℓ^{th} subband as follows:

$$n_{\ell}^{\mathrm{2D}} = m_{\ell}^{\mathrm{eff}}\frac{m_e}{2\pi\hbar^2}k_BT\ln\left[1+\exp\left(\frac{E_{\ell}-\mu}{k_BT}\right)\right]. \tag{9}$$

Here μ is the chemical potential of the system. And the spatial distribution of holes (with spin σ) in the spin-polarized ℓ^{th} subband is given by $n_{\ell}^{\sigma}(z)=\Sigma_{j=1}^{6}n_{\ell}^{\mathrm{2D}}|\varphi_{j\ell}(z)|^2|a_j^{\sigma}|^2$, where a_j^{σ} is the spin σ component of Bloch functions $u_{j0}=\Sigma_{\sigma}a_j^{\sigma}|\sigma\rangle$. Then the spin distribution of holes is $n_{\sigma}(z)=\Sigma_{\ell}n_{\ell}^{\sigma}(z)$. The spontaneous magnetization of Mn impurities becomes $M=-x_{\mathrm{eff}}N_0g_{\mathrm{Mn}}\mu_B\langle S_y\rangle$.[11] Here g_{Mn} and μ_B are the

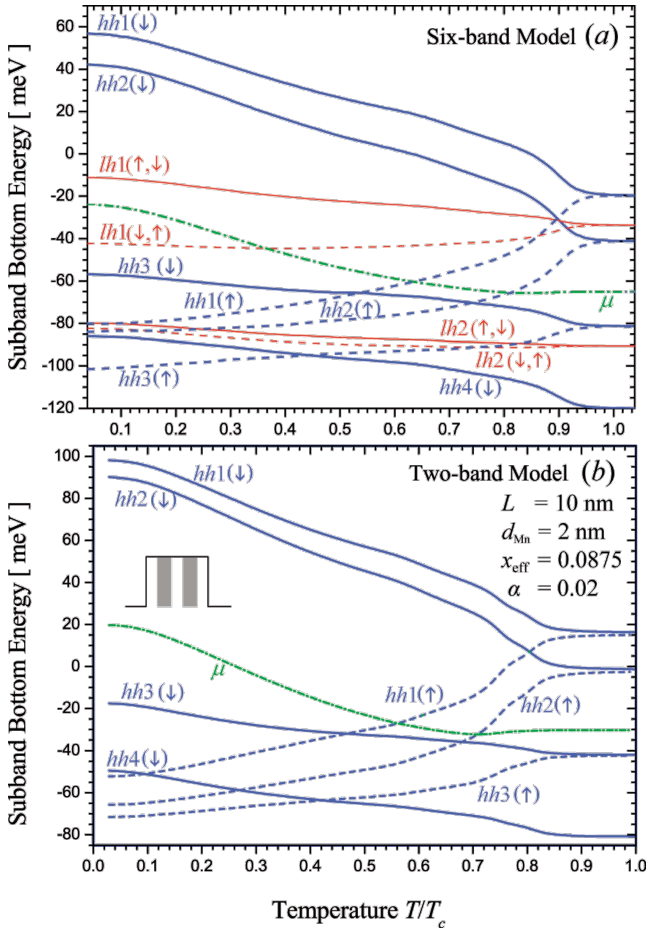

FIG. 2. (Color online) The temperature dependence of subband structure of dilute (Ga,Mn)As QWs in (a) six-band and (b) two-band calculations when Mn ions are doped near the central part in the QW. hh and (lh) denotes heavy-hole (light-hole) states in the valence band and μ is chemical potential. And $\downarrow$ ($\uparrow$) indicates the majority (minority) spin state.

gyromagnetic ratio of Mn ion and Bohr magneton, respectively.

III. RESULT AND DISCUSSION

Following the prescription described in the preceding section, we evaluate the spin-resolved subband structure $\{E_\ell, \varphi_{i\ell}\}$ and magnetization in AlGaAs/(Ga,Mn)As/AlGaAs QWs. In order to study the variation in magnetic properties for different Mn-doping profiles, the effective number of Mn impurities is kept constant in GaAs well. So, the x_{eff} is adjusted in accord with the total width L_{M} of Mn-doped layers. In actual calculation, we took x_{eff}=0.035 and x_{eff}=0.0875 for uniform (L_{M}=10 nm) and selective (L_{M}=4 nm) Mn-doped cases, respectively. For selective Mn doping, the width of each piece of magnetic layer in the well is d_{Mn}=2 nm and L_{M}=2d_{Mn} (see Fig. 1). We also investigate coupling effect of heavy-hole, light-hole, and split-off bands for a given selectively Mn-doped QW.

Figures 2(a) and 2(b) show the temperature dependence of subband bottom energies E_ℓ in six-band and two-band models, respectively, for the case that Mn impurities are doped near the central part of the GaAs QW. The doping efficiency α is taken to be 0.02, which is about the same order as that estimated in experiment.[17] The temperature is scaled in units of T_c of the structure. Here the thick solid and dashed (blue) lines indicate the subband bottom energies of hh states, and the thin solid and dashed (red) lines denote the result of the lh states. The dash-dot (green) line is the chemical potential μ. The subband states above the chemical potential μ are occupied by itinerant band carriers (holes). In six-band calculation shown in Fig. 2(a), the lh subband states, which are neglected in two-band model, are occupied by holes. Although the hh subband states are spin polarized, the lh subband states are spin mixed as shown in Fig. 2(a). The difference between lh1 subband bottoms and chemical potential μ is proportional to hole concentration of the lh1 subbands. We note that the hole concentrations of the lh1 subbands are increased as the temperature increases. Because the spin direction of lh subband is different from that of hh hole, spin polarization ζ of the system is evaluated to be reduced in the six-band model in comparison with the case of the two-band model. In our calculation, the ratio $n_{\text{lh}}^{\text{2D}}/n_{\text{hh}}^{\text{2D}}$ is calculated to be 0.065 in the temperature region of $T/T_c \sim 1.0$, in which $n_{\text{lh}}^{\text{2D}}$ has the largest value.

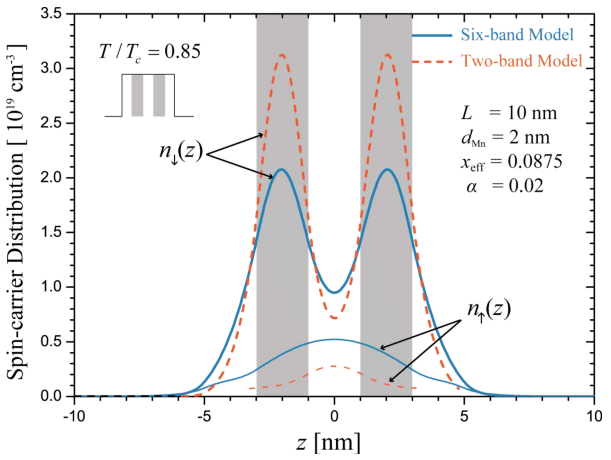

FIG. 3. (Color online) Spin-resolved carrier distributions $n_\sigma(z)$ for the case that Mn impurities are selectively doped near the central part in the QW.

Hence, the hole concentration of the lh subbands is relatively small in comparison with hole concentration of hh subbands, but its influence on the spin polarization and spatial distribution of holes is not negligible. As an example, Fig. 3 illustrates the spin-resolved carrier distribution of holes in the QW at T/T_c=0.85. Here the thick and thin solid (blue) lines indicate the spatial distribution $n_\sigma(z)$ of majority ($\downarrow$) and minority ($\uparrow$) spin holes, respectively, obtained in six-band model, and the dashed (red) lines are the result of two-band model. We note that the spin polarization and number of holes in the magnetic layers (gray regions) are overestimated in the two-band calculation. Here, we observe that the variation in the spatial distribution of the holes occupying subband states is in accord with the subband structure shown in Fig. 2.

Figure 4 shows the temperature dependence of spontaneous magnetization for three different Mn-doping profiles in a

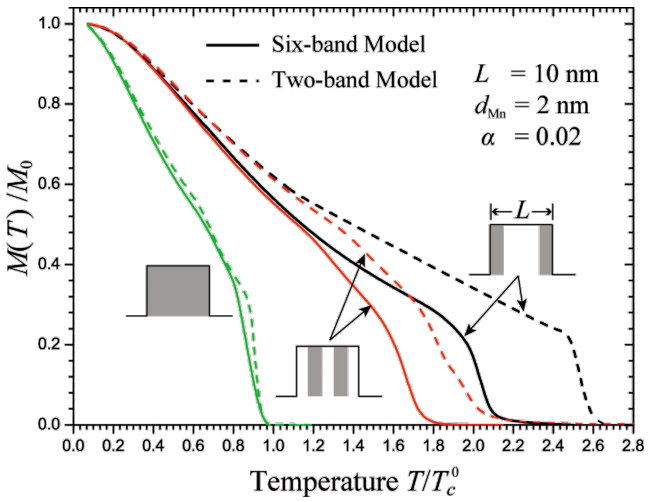

FIG. 4. (Color online) Spontaneous magnetization for three different Mn-doping profiles. Mn-doped regions in QW are shaded in the insets. The solid (dashed) lines indicate the results of six-band (two-band) model calculation.

QW of width $L=10$ nm. Corresponding profiles are displayed in the insets with shades showing Mn-doped regions. The magnetization $M(T)$ and the temperature T are measured in units of M_0 and T_c^0, the saturation value of $M(T)$ and Curie temperature for the case of uniformly doped Mn impurities in six-band model. We note that selective Mn doping enhances the ferromagnetic tendency of the system in comparison with uniform doping and the case of Mn impurities doped selectively near the well edges shows higher value of T_c than the case of Mn impurities doped near the central part of the well. Our result shows that, for the former case, the kinetic exchange interaction between holes and Mn ions become large to result in an effective potential $V_{\text{eff}}(z)$, which distributes most of the carriers in the magnetic region doped with Mn. Then the spatial overlap between Mn impurities and holes is greatly enhanced and the value of $M(T)$ is more sensitive to the changes in ζ and $n_\sigma(z)$ of itinerant carriers compared to the case of uniform Mn doping. We conjecture that this phenomenon should appear more distinctly as the number of holes overlapping with Mn impurities increases. We also observe that the discrepancy between spontaneous magnetizations $M(T)$ from two-band and six-band calculations become large as the temperature is increased, especially for the structures with magnetic layers near the well edges. Main reason of the discrepancy between two model calculations is directly related whether light-hole and split-off subband states are occupied by carriers. This observation appears more clearly near the critical temperature.

In summary, we studied spin-resolved subband structures and spontaneous magnetization of diluted (Ga,Mn)As QWs taking into account of the coupling effect of valence bands. We find that selective Mn doping in GaAs QW enhances the Curie temperature T_c significantly. Although the number of holes in lh subbands is relatively small in comparison with those of hh subbands, they considerably influence magnetic properties as the temperature approaches the Curie temperature. Experimental confirmation of our finding in DMS (Ga,Mn)As QW structure would be of great use to realization of practical operation temperature of DMS material in spintronics applications.

ACKNOWLEDGMENT

This work was supported in part by the Grant No. KRF-2006-005-J02804.

*neverend@pusan.ac.kr
†ksyi@pusan.ac.kr

[1] K. C. Ku, S. J. Potashnik, R. F. Wang, S. H. Chun, P. Schiffer, N. Samarth, M. J. Seong, A. Mascarenhas, E. Johnston-Halperin, R. C. Myers, A. C. Gossard, and D. D. Awschalom, Appl. Phys. Lett. **82**, 2302 (2003).
[2] T. Jungwirth, K. Y. Wang, J. Mašek, K. W. Edmonds, J. König, J. Sinova, M. Polini, N. A. Goncharuk, A. H. MacDonald, M. Sawicki, A. W. Rushforth, R. P. Campion, L. X. Zhao, C. T. Foxon, and B. L. Gallagher, Phys. Rev. B **72**, 165204 (2005).
[3] M. Wang, R. P. Campion, A. W. Rushforth, K. W. Edmonds, C. T. Foxon, and B. L. Gallagher, Appl. Phys. Lett. **93**, 132103 (2008).
[4] B. Lee, T. Jungwirth, and A. H. MacDonald, Phys. Rev. B **61**, 15606 (2000).
[5] H. J. Kim and K. S. Yi, Phys. Rev. B **65**, 193310 (2002).
[6] H. J. Kim and K. S. Yi, Physica E **32**, 403 (2006); J. Korean Phys. Soc. **45**, S559 (2004).
[7] A. M. Nazmul, T. Amemiya, Y. Shuto, S. Sugahara, and M. Tanaka, Phys. Rev. Lett. **95**, 017201 (2005).
[8] D. Kolovos-Vellianitis, C. Herrmann, A. Trampert, L. Däweritz, and K. H. Ploog, J. Vac. Sci. Technol. B **24**, 1734 (2006).
[9] T. Jungwirth, J. Sinova, J. Mašek, J. Kučera, and A. H. MacDonald, Rev. Mod. Phys. **78**, 809 (2006).
[10] O. Gunnarsson and B. I. Lundqvist, Phys. Rev. B **13**, 4274 (1976).
[11] J. K. Furdyna, J. Appl. Phys. **64**, R29 (1988).
[12] G. Bastard, *Wave Mechanics Applied to Semiconductor Heterostructure* (Holsted Press-John Wiley & Sons, Inc., New York, 1988), p. 84.
[13] C. F. Gerald and P. O. Wheatley, *Applied Numerical Analysis* (Addison Wesley Longman, London, 1999), p. 533.
[14] S. H. Chuang, *Physics of Optoelectronic Devices* (John Wiley & Sons, Inc, New York, 1995), p. 140.
[15] T. Dietl, H. Ohno, and F. Matsukura, Phys. Rev. B **63**, 195205 (2001).
[16] O. Madelung, *Semiconductors-Basic Data* (Springer, New York, 1996), p. 103.
[17] See, for example, S. Chung, H. C. Kim, S. Lee, X. Liu, and J. K. Furdyna, Solid State Commun. **149**, 1739 (2009).